Highly conserved tyrosine stabilizes the active state of rhodopsin

Joseph A. Goncalves[a], Kieron South[b], Shivani Ahuja[c], Ekaterina Zaitseva[d], Chikwado A. Opefi[b], Markus Eilers[a], Reiner Vogel[d], Philip J. Reeves[b], and Steven O. Smith[a,1]

[a]Department of Biochemistry and Cell Biology, Stony Brook University, Stony Brook, NY 11794; [b]Department of Biological Sciences, University of Essex, Wivenhoe Park, Colchester, Essex C04 3SQ, United Kingdom; [c]Department of Physics and Astronomy, Stony Brook University, Stony Brook, NY 11794; and [d]Biophysics Section, Institute of Molecular Medicine and Cell Research, Albert-Ludwigs-University, Freiburg, Hermann Herder Strasse, D-79104 Freiburg, Germany

Edited by Richard Henderson, Medical Research Council Laboratory of Molecular Biology, Cambridge, United Kingdom, and approved September 23, 2010 (received for review June 30, 2010)

Light-induced isomerization of the 11-*cis*-retinal chromophore in the visual pigment rhodopsin triggers displacement of the second extracellular loop (EL2) and motion of transmembrane helices H5, H6, and H7 leading to the active intermediate metarhodopsin II (Meta II). We describe solid-state NMR measurements of rhodopsin and Meta II that target the molecular contacts in the region of the ionic lock involving these three helices. We show that a contact between Arg135$^{3.50}$ and Met257$^{6.40}$ forms in Meta II, consistent with the outward rotation of H6 and breaking of the dark-state Glu134$^{3.49}$-Arg135$^{3.50}$-Glu247$^{6.30}$ ionic lock. We also show that Tyr223$^{5.58}$ and Tyr306$^{7.53}$ form molecular contacts with Met257$^{6.40}$. Together these results reveal that the crystal structure of opsin in the region of the ionic lock reflects the active state of the receptor. We further demonstrate that Tyr223$^{5.58}$ and Ala132$^{3.47}$ in Meta II stabilize helix H5 in an active orientation. Mutation of Tyr223$^{5.58}$ to phenylalanine or mutation of Ala132$^{3.47}$ to leucine decreases the lifetime of the Meta II intermediate. Furthermore, the Y223F mutation is coupled to structural changes in EL2. In contrast, mutation of Tyr306$^{7.53}$ to phenylalanine shows only a moderate influence on the Meta II lifetime and is not coupled to EL2.

G protein-coupled receptor | solid-state NMR spectroscopy | ERY motif

Rhodopsin, the vertebrate photoreceptor for vision under dim light, belongs to the large, pharmaceutically important superfamily of G protein-coupled receptors (GPCRs). The photoreactive chromophore in rhodopsin is the 11-*cis*-isomer of retinal, which is covalently linked to Lys296$^{7.43}$ [superscripts denote Ballesteros–Weinstein numbering (1)] on the intradiscal (or extracellular) side of the receptor. Absorption of light drives the 11-*cis*- to *trans*-isomerization of the retinal within a tight binding pocket. The conformational changes that occur in this process must be transmitted through the membrane-spanning portion of the bilayer to the intracellular surface in order to open up the binding site for the heterotrimeric G protein, transducin. The crystal structure of the dark, inactive state of the visual pigment rhodopsin (2) reveals a tightly packed bundle of seven transmembrane (TM) helices but offers few clues as to how the helices move upon light activation.

Site-directed spin-labeling studies by Hubbell and coworkers (3, 4) showed that the largest change in the seven-TM-helix bundle involves an outward rotation of helix H6, consistent with an increase in volume of the receptor upon activation (5). The challenge for obtaining a high-resolution structure of the active metarhodopsin II (Meta II) intermediate has been that light activation causes the dark-state crystals of rhodopsin to dissolve (6), suggesting that the structural changes are sufficiently large to disrupt crystal packing. Salom et al. (7) were able to determine the crystal structure to 4.15-Å resolution of a photointermediate of rhodopsin containing retinal with a deprotonated Schiff base (SB) (7). The structure did not exhibit the large helix motions characteristic of the activated receptor, suggesting that this intermediate corresponds to the Meta II substate (Meta IIa) formed prior to helix motion (8).

More recently, Park et al. determined the structure of opsin (9). Opsin is formed when the Meta II intermediate decays and releases the agonist *all-trans*-retinal from the retinal-binding site. Opsin has low (≤1%), but detectable, basal activity in rod outer segment cell membranes (10). At pH 4, FTIR difference spectra of opsin exhibit vibrational bands characteristic of Meta II (11), suggesting that opsin adopts an active conformation. The crystals of opsin obtained at pH 6 appear to retain many features characteristic of the active state (Fig. 1). In fact, the most recent crystal structure of opsin (12) contains the bound C-terminal peptide of the Gα subunit of transducin in a conformation similar to that observed in solution NMR studies on the activated Meta II intermediate (13, 14).

One of the most striking features of the opsin structure is that the ionic lock involving Glu134$^{3.49}$-Arg135$^{3.50}$ of the conserved ERY sequence on H3 and Glu247$^{6.30}$ on H6 is disrupted (Fig. 1*B*). The opsin structure reveals an outward motion of H6, similar in magnitude (~6 Å) to the change observed by spin-labeling studies (3). Arg135$^{3.50}$ is extended toward Met257$^{6.40}$, Tyr223$^{5.58}$, and Tyr306$^{7.53}$. Both Tyr223$^{5.58}$ and Tyr306$^{7.53}$ have strong sequence identity in the class A GPCRs. Tyr306$^{7.53}$ is part of a cluster of highly conserved residues on the cytoplasmic side of H7 and is thought to impart stability of the inactive receptor (15). Tyr223$^{5.58}$ is unusual in that it is oriented away from the helical bundle in the inactive, dark receptor but rotates in toward the ionic lock in the opsin crystal structure. Whereas Tyr306$^{7.53}$ of the NPxxY sequence has been characterized extensively, the only evidence that Tyr223$^{5.58}$ plays a critical role in receptor activation comes from the opsin structure.

Solid-state NMR spectroscopy provides a unique way of following the structural transitions from rhodopsin to Meta II (16, 17) by allowing measurements in a fluid membrane environment, which facilitates the conformational changes associated with the formation of Meta II. The work to date has focused on the retinal-binding pocket. Here, we use solid-state NMR to determine the structure of the ionic lock in Meta II and fluorescence spectroscopy to characterize the rates of Meta II decay in mutants of rhodopsin where three highly conserved tyrosines (Tyr136$^{3.51}$, Tyr223$^{5.58}$, and Tyr306$^{7.53}$) on the cytoplasmic side of the receptor have been sequentially mutated to phenylalanine. Our experiments on Meta II stability and transducin activation

Author contributions: J.A.G., S.A., M.E., and S.O.S. designed research; J.A.G., K.S., S.A., E.Z., C.A.O., M.E., R.V., and P.J.R. performed research; E.Z., C.A.O., R.V., and P.J.R. contributed new reagents/analytic tools; J.A.G., K.S., S.A., E.Z., M.E., R.V., P.J.R., and S.O.S. analyzed data; and J.A.G., M.E., R.V., P.J.R., and S.O.S. wrote the paper.

The authors declare no conflict of interest.

This article is a PNAS Direct Submission.

[1]To whom correspondence should be addressed. E-mail: steven.o.smith@sunysb.edu.

This article contains supporting information online at www.pnas.org/lookup/suppl/doi:10.1073/pnas.1009405107/-/DCSupplemental.

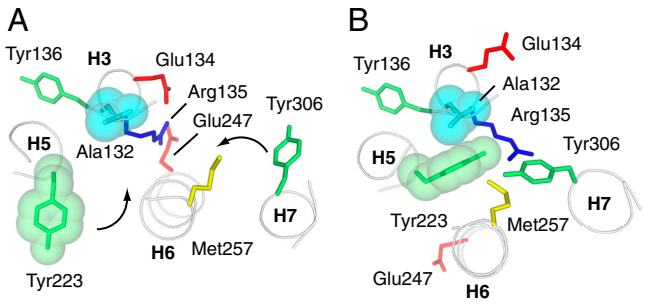

Fig. 1. Comparison of the rhodopsin and opsin crystal structures in the region of the ionic lock. (*A*) Structure of rhodopsin in the region of the ionic lock as viewed from the extracellular surface. (*B*) Structure of opsin at low pH in the same orientation as in *A*. The side chains of Tyr223$^{5.58}$ and Tyr306$^{7.53}$ are rotated inward toward the helical bundle where they are within hydrogen-bonding distance of Arg135$^{3.50}$. Ala132$^{3.47}$ is the most highly group-conserved residue in class A GPCRs.

provide insights into the roles of these three conserved tyrosines. We show that Tyr223$^{5.58}$ has a more substantial contribution to the stability of Meta II and transducin activation than either Tyr136$^{3.51}$ or Tyr306$^{7.53}$.

Results

The Open State of the Ionic Lock in Meta II. The outward rotation of H6 observed in the opsin crystal structure places the side chain of Met257$^{6.40}$ in close proximity to Arg135$^{3.50}$. The ^{15}N chemical shifts of the Nη_1, Nη_2, and Nε side-chain nitrogens and the ^{13}C chemical shift of the Cζ carbon were measured to address the changes in the environment of Arg135$^{3.50}$ upon Meta II formation. The arginine ^{15}N chemical shifts are sensitive to the protonation state and environment of the guanidinium group (18), and one can envisage that when the interactions between Glu134$^{3.49}$, Arg135$^{3.50}$, and Glu247$^{6.30}$ are broken, Arg135$^{3.50}$ undergoes a change in electrostatic environment.

The ^{15}N and ^{13}C spectra of arginine-labeled rhodopsin and Meta II are presented in Fig. S1. There is no chemical shift resolution in the ^{15}N resonances of the arginine Nη_1, Nη_2, and Nε nitrogens in either rhodopsin or Meta II, and there is only a slight (<1 ppm) shift in the ^{13}Cζ resonance. The lack of significant changes indicates that the protonation state of Arg135$^{3.50}$ has not changed and suggests that the electrostatic environment surrounding Arg135$^{3.50}$ is similar in the inactive and active states. These results suggest that either there are no large changes in the receptor structure as suggested by the crystal structure of the rhodopsin photoproduct with a deprotonated retinal SB or that disruption of the full charge–charge interactions within the Glu134$^{3.49}$-Arg135$^{3.50}$-Glu247$^{6.30}$ ionic lock are compensated by partial charge interactions that result in no substantial change in the ^{15}N or ^{13}C chemical shifts of Arg135$^{3.50}$.

In contrast to the lack of chemical shift changes in arginines, there are substantial changes observed in the chemical shifts of methionines. Fig. 2*A* presents the ^{13}C NMR difference spectrum between ^{13}Cε-Met-labeled rhodopsin and Meta II. The negative ^{13}C resonance at ~15 ppm can tentatively be assigned to Met257$^{6.40}$ in Meta II on the basis of its sensitivity to mutation of Tyr223$^{5.58}$ and Tyr306$^{7.53}$. To test for a direct Arg135$^{3.50}$-Met257$^{6.40}$ interaction in Meta II, we labeled rhodopsin with U-^{13}C, ^{15}N-Arg, and ^{13}Cε-Met and measured internuclear Arg-Met distances by using 2D ^{13}C dipolar-assisted rotational resonance (DARR) NMR. We do not observe Arg ^{13}Cζ-Met ^{13}Cε crosspeaks in the 2D DARR NMR spectrum of rhodopsin (Fig. 2*B*, black line) consistent with the rhodopsin crystal structure where no Arg Cζ-Met Cε carbon pairs are closer than ~6 Å. In contrast, an Arg Cζ-Met Cε crosspeak is observed in Meta II (Fig. 2*B*, red line) that we tentatively assign to Arg135$^{3.50}$-Met257$^{6.40}$. In the opsin crystal structure, the Arg135$^{3.50}$ Cζ-Met257$^{6.40}$ Cε distance is 4.6 Å, within the range of this

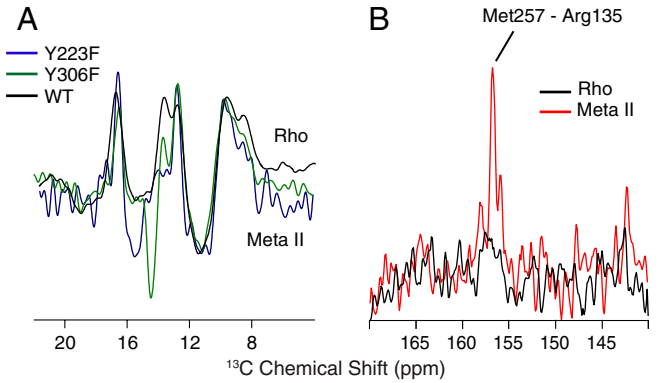

Fig. 2. Arg135$^{3.50}$-Met257$^{6.40}$ contacts in Meta II. (*A*) ^{13}C NMR difference spectra between rhodopsin and Meta II in the region of ^{13}Cε-methionine of the wild-type receptor (black line) and the Y223F (blue line) and Y306F (green line) mutants. The ^{13}Cε-Met257 resonance at 14.7 ppm exhibits a crosspeak with ^{13}Cζ-Arg135$^{3.50}$ in Meta II (see *B*). Mutation of either Tyr223$^{5.58}$ or Tyr306$^{7.53}$ leads to slight shifts in the ^{13}Cε-Met257$^{6.40}$ resonance. (*B*) Rows through the Met-Cε diagonal resonance are shown from 2D ^{13}C DARR NMR spectra of rhodopsin (black line) and Meta II (red line) labeled with ^{13}Cε-methionine and ^{13}Cζ-arginine. A strong crosspeak is observed in Meta II at the ^{13}Cε-Met chemical shift of 14.7 ppm and the ^{13}Cζ-Arg135$^{3.50}$ chemical shift of 156.8 ppm. The crosspeak is assigned to a close through-space contact between Arg135$^{3.50}$ and Met257$^{6.40}$. Arg-Met crosspeaks are not observed in the spectrum of dark rhodopsin (black line).

experiment. The putative Arg135$^{3.50}$-Met257$^{6.40}$ contact in Meta II correlates with the position of these two residues in the opsin crystal structure. The next closest Arg-Met pair is Arg135$^{3.50}$ and Met253$^{6.36}$, whose Cζ–Cε distance is 6.5 Å.

To further characterize the local environment of Arg135$^{3.50}$ in Meta II, we targeted the two conserved tyrosines (Tyr223$^{5.58}$ and Tyr306$^{7.53}$) that appear to stabilize the ionic lock in an open conformation (Fig. 1*B*). The side-chain hydroxyl groups of Tyr223$^{5.58}$ and Tyr306$^{7.53}$ may act in concert to preserve the dark-state electrostatic environment of Arg135$^{3.50}$.

Fig. 3 presents difference spectra generated by subtraction of the spectrum of wild-type rhodopsin from the spectrum of one of three tyrosine mutants (Y136F, Y223F, or Y306F). Only the region of the ^{13}Cζ tyrosine resonances is shown. These spectra allow us to directly assign the ^{13}Cζ tyrosine chemical shifts in rhodopsin and in Meta II. Both the Tyr223$^{5.58}$ and Tyr306$^{7.53}$ resonances shift downfield slightly upon activation to 156.2 and 155.9 ppm, respectively, reflecting an increase in hydrogen bonding of the ^{13}Cζ-OH group and indicating that both tyrosines are protonated and in a similar environment in Meta II. For comparison, the difference spectrum of Y136F is shown in Fig. 3*A*. The ^{13}Cζ chemical shift of Tyr136$^{3.51}$ does not change upon activation.

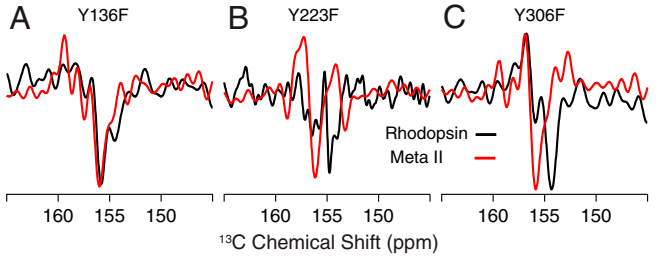

Fig. 3. ^{13}Cζ chemical shifts of Tyr136$^{3.51}$, Tyr223$^{5.58}$, and Tyr306$^{7.53}$ in rhodopsin and Meta II. Difference spectra obtained between rhodopsin (black line) and Meta II (red line) for the three tyrosine mutants: Y306F, Y223F, and Y136F. The difference spectra are taken between the wild-type protein and the mutant in order to reveal the frequency of the ^{13}Cζ resonance. Tyr223$^{5.58}$ and Tyr306$^{7.53}$ both exhibit downfield changes in chemical shift between rhodopsin and Meta II. The ^{13}Cζ chemical shift of Tyr136$^{3.51}$ is not appreciably altered upon conversion to Meta II.

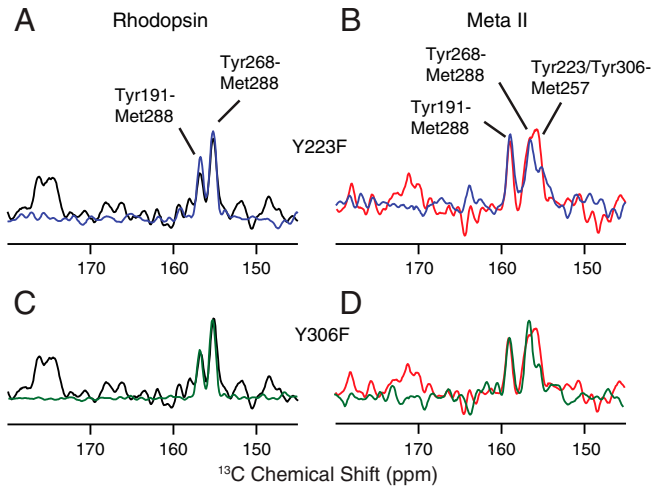

Fig. 4. Tyr223$^{5.58}$-Met257$^{6.40}$ and Tyr306$^{7.53}$-Met257$^{6.40}$ contacts in Meta II. Rows through the Met-Cε diagonal resonance are shown from 2D ^{13}C DARR NMR spectra of rhodopsin (black line) and Meta II (red line) labeled with ^{13}Cζ-tyrosine and ^{13}Cε-methionine. The rhodopsin and Meta II rows are overlaid with the corresponding rows obtained of the Y223F (blue line) and Y306F (green line) mutants in order to determine if either of these tyrosines contact Met257$^{6.40}$ in Meta II. Upon mutation of Tyr223$^{5.58}$ or Tyr306$^{7.53}$, there is loss of intensity of the crosspeak at 156 ppm, consistent with these tyrosines having similar chemical shifts and interacting with Met257$^{6.40}$ in Meta II.

To establish if direct Tyr223$^{5.58}$-Met257$^{6.40}$ and Tyr306$^{7.53}$-Met257$^{6.40}$ contacts occur in Meta II, we obtained 2D DARR NMR spectra of wild-type (black line) and mutant (red line) rhodopsin ^{13}C labeled at ^{13}Cε-methionine and ^{13}Cζ-tyrosine (Fig. 4). In rhodopsin, rows taken through the Met-Cε diagonal resonance of the DARR spectrum reveal crosspeaks between Tyr191^{EL2}-Met288$^{7.35}$ at 156.8 ppm and Tyr268$^{6.51}$-Met288$^{7.35}$ at 155.2 ppm (17). In the dark, both Tyr191^{EL2} and Tyr268$^{6.51}$ participate in a network of hydrogen-bonding interactions that help to position the second extracellular loop (EL2) deep within the retinal-binding pocket. The observation that neither of these crosspeaks change upon substitution of Tyr223$^{5.58}$ or Tyr306$^{7.53}$ is consistent with a native-like inactive conformation being adopted by both mutants.

In the rows corresponding to wild-type Meta II, a shoulder appears at ~156 ppm (Fig. 4 *B* and *D*, red line), consistent with the chemical shifts of Tyr223$^{5.58}$ and Tyr306$^{7.53}$ observed in Fig. 3. This shoulder is lost upon mutation of either Tyr306$^{7.53}$ or Tyr223$^{5.58}$. These data confirm the proximity of Met257$^{6.40}$ to both Tyr306$^{7.53}$ and Tyr223$^{5.58}$ in Meta II. In turn, these results place both tyrosine side chains in close proximity to the active state position of Arg135$^{3.50}$.

Tyr223$^{5.58}$ Stabilizes the Active Meta II Intermediate. The lack of chemical shift changes in the arginine ^{15}N and ^{13}C resonances (Fig. S1) suggests that the electrostatic environment around Arg135$^{3.50}$ does not change appreciably upon activation. This observation along with the NMR structural data on Meta II showing that Tyr223$^{5.58}$ and Tyr306$^{7.53}$ surround Arg135$^{3.50}$ suggests that these residues interact with one another and contribute to the stabilization of the active Meta II conformation. To address the role of these tyrosines in Meta II stability, we monitored the decay of Meta II by fluorescence spectroscopy.

Fig. 5 presents fluorescence data on the decay of Meta II in wild-type rhodopsin and the Y223F mutant. For wild-type rhodopsin, fluorescence increases in the transition from Meta II to opsin. The fluorescence changes are associated with a loss of an interaction between Trp265$^{6.48}$ and the retinal chromophore that quenches tryptophan fluorescence in Meta II (19). When plotted as a function of time after illumination, the fluorescence

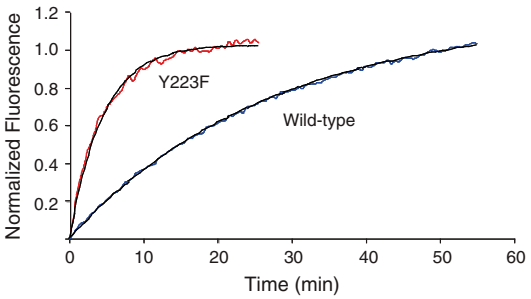

Fig. 5. Comparison of Meta II decay in wild-type and Y223F rhodopsin. The fluorescence emission at 330 nm from wild-type rhodopsin and the Y223F mutant is plotted as a function of time after light activation. Normalized Meta II decay rates were calculated by fitting the data to a first-order decay function. There is a 4.7-fold increase in the rate of Meta II decay upon mutation of Tyr223$^{5.58}$ (Table 1).

increase can be fitted to a single exponential function. For the Y223F mutant, the fluorescence intensity reaches a maximum after 400 s corresponding to a fivefold increase in the Meta II decay relative to the wild-type receptor. For comparison, mutation of either Tyr136$^{3.51}$ or Tyr306$^{7.53}$ to phenylalanine increases Meta II decay by less than a factor of 2 (Table 1). These data suggest that Tyr223$^{5.58}$ has a greater contribution to Meta II stability than either Tyr136$^{3.51}$ or Tyr306$^{7.53}$.

We tested the ability of the three tyrosine mutants (Y136F, Y223F, and Y306F) to activate the G protein transducin (Table 1). For the Y223F mutant, there is a large decrease in both the initial rate of transducin activation and the maximum level of activation as compared to wild-type rhodopsin (as revealed by the normalized fluorescence increase, Table 1), consistent with the rapid hydrolysis of the *all-trans*-retinal SB in the formation of opsin.

For the Y136F mutant, we observed that Meta II stability was similar to wild-type rhodopsin. However, the initial rate of transducin activity was significantly (1.5×) higher. In a previous study, it was found that a nearby rhodopsin retinitis pigmentosa mutant (V137M) also displayed elevated (1.25×) initial rates of transducin activation (20). In the case of Y136F, we do not observe an associated increase in SB hydrolysis, suggesting that the structural consequences of this mutation are limited to the cytoplasmic side of the receptor. The analogous tyrosine has been the focus of several studies in other class A GPCRs, such as the vasopressin receptor (21) and CCR3 (22), where a conservative substitution blocks signaling while maintaining native-like ligand affinity.

Further support for the role of Tyr223$^{5.58}$ in stabilizing Meta II comes from FTIR measurements obtained at lower temperature (*Supporting Information*). Analysis of vibrational band intensities characteristic of Meta I and Meta II shows that the Meta I⇔Meta II equilibrium is strongly shifted to the Meta I state in the Y223F mutant (Fig. S2).

Table 1. The normalized rates of Meta II decay and transducin activation of Tyr136$^{3.51}$, Tyr223$^{5.58}$, Tyr306$^{7.53}$, and Ala132$^{3.47}$ mutants at 20 °C

	Meta II decay (n = 3)		Transducin activation (n = 2)	
	Half-life, min	Normalized decay rate, % of wild type	Normalized initial rate, % of wild type	Normalized fluorescence increase, % of wild type
Wild-type	14.8 ± 0.3*	100 ± 2.1*	100 ± 7.1*	100 ± 4.1*
Y136F	12.5 ± 0.9	118 ± 8.6	149 ± 16.9	106 ± 3.4
Y223F	3.2 ± 0.2	466 ± 29.0	6 ± 1.5	5 ± 2.9
Y306F	10.5 ± 0.6	140 ± 8.1	84 ± 7.4	72 ± 2.2
A132L	3.8 ± 0.3	386 ± 31.0	69 ± 1.2	34 ± 6.2
A132S	9.3 ± 1.2	159 ± 20.9	31 ± 8.2	63 ± 2.8

*Mean ± standard error.

Ala132$^{3.47}$ Orients Tyr223$^{5.58}$ in Meta II. One helix turn from Arg135$^{3.50}$ into the receptor core is the group-conserved Ala132$^{3.47}$. Group-conserved residues generally have low conservation when considered individually but are highly conserved when considered as a group consisting of amino acids with small or weakly polar side chains, namely, Ala, Gly, Ser, Thr, and Cys. These residues have a high propensity to mediate TM-helix interactions (23) and have been shown to allow interaction of the signature residues in the class A GPCRs (24). Position 3.47 has the highest level of group conservation within this group (99%). In the crystal structure of opsin, the large rotation of Tyr223$^{5.58}$ places its aromatic side chain in van der Waals contact with Ala132$^{3.47}$. The rapid decay of Meta II upon mutation of Tyr223$^{5.58}$ is similar to that previously observed for mutation of Glu122$^{3.37}$ (25). Glu122$^{3.37}$ hydrogen bonds with His211$^{5.46}$ on the extracellular side of the receptor in Meta II and is thought to hold H5 in an active orientation (26). The His211$^{5.46}$-Glu122$^{3.37}$ pair is conserved in the high-sensitivity rod cell pigments and distinguishes them from the lower-sensitivity cone pigments. The question arises as to whether there is a similar pairwise stabilizing interaction between Tyr223$^{5.58}$ and Ala132$^{3.47}$ on the intracellular side of the receptor.

To test this hypothesis, we mutated Ala132$^{3.47}$ to Leu and Ser and measured Meta II decay by tryptophan fluorescence. These data reveal an increased rate of Meta II decay (Table 1) suggesting that a larger side chain at position 132$^{3.47}$ does not allow Tyr223$^{5.58}$ to form a stabilizing interaction with Arg135$^{3.50}$. The observed increase in the rate of Meta II decay in the A132L mutant is consistent with a lower activity of the Meta II state.

The Y223F Mutation Causes Structural Changes in EL2. The shift in the Meta I⇔Meta II equilibrium and faster Meta II decay of the Y223F mutant suggest that the changes introduced by this mutation are allosterically coupled to the extracellular side of the receptor. This hypothesis is in agreement with the coupling of EL2 and H5 motion during activation (17). Meta II decay is defined by hydrolysis of the SB. There are several amino acids on or near EL2 on the extracellular side of rhodopsin that can modulate SB hydrolysis (27), including Glu113$^{3.28}$ (28). We propose that the position of EL2 is linked to the position of Glu113$^{3.28}$ and SB hydrolysis.

To characterize whether the mutation of Tyr223$^{5.58}$ or Tyr306$^{7.53}$ is coupled to structural changes in EL2, we expressed the Y223F and Y306F mutants with $^{13}C\beta$-labeled cysteine. The cysteine Cβ-spectrum provides a probe for changes in the highly conserved Cys110$^{3.25}$ and Cys187^{EL2} disulfide bond. The β-carbon resonances in cysteines are observed in a unique chemical shift window (34–50 ppm) and are sensitive to the secondary structure: 34–43 ppm for α-helices and 36–50 ppm for β-sheets. We previously observed strong crosspeaks between the Cys110$^{3.25}$-Cys187^{EL2} β-carbon resonances at 36.4 and 46.8 ppm in the dark, respectively (17). These resonances do not change position in the Y223F or Y306F rhodopsin spectra.

Fig. 6 presents rows from the 2D DARR NMR spectra of Meta II of the Y223F (blue line) and Y306F (green line) mutants labeled with $^{13}C\beta$-cysteine as compared to wild-type Meta II (red line). In contrast to the comparison with dark rhodopsin, there is a shift of the Cys187^{EL2} resonance in the Meta II spectrum of the Y223F mutant compared to wild-type Meta II. In wild-type Meta II, the Cys187^{EL2} resonance shifts to 50.1 ppm because of a change in the conformation of EL2, whereas the chemical shift of Cys110$^{3.25}$ on helix H3 does not change (17). In the Y223F mutant, the Cys187^{EL2} resonance moves upfield to 48.2 ppm (Fig. 6*A*). Fig. 6*C* shows the crosspeak associated with Cys110$^{3.25}$. This crosspeak does not shift in the Y223F mutant, confirming that the influence of the mutation is localized to EL2. In the Y306F mutant (Figs. 6 *B* and *D*), the crosspeaks associated with Cys110$^{3.25}$ and Cys187^{EL2} are at the same position as in wild-type Meta II, indicating that there is no coupling between the NPxxY sequence and the conserved cysteine disulfide.

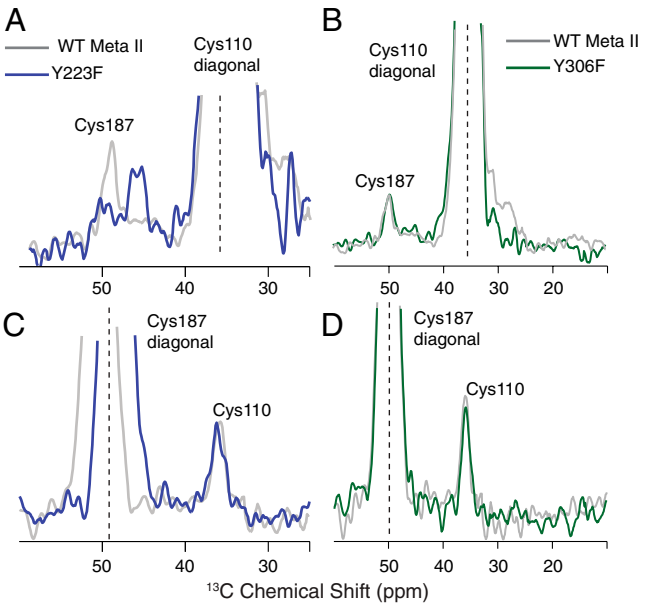

Fig. 6. Coupling of H5 to EL2 motion in the Y223F mutant of Meta II. Rows extracted from 2D ^{13}C DARR NMR spectra acquired of the activated Meta II state of wild-type rhodopsin (gray line) and the Y223F (blue line) and Y306F (green line) mutants. The rows show the Cβ region of Cys110$^{3.25}$ and Cys187^{EL2} and were taken through the diagonal resonances of Cys110$^{3.25}$ (*A* and *B*) and Cys187^{EL2} (*C* and *D*). Mutation of Tyr223$^{5.58}$ alters the chemical shift of Cys187^{EL2} with respect to wild-type rhodopsin (gray line). However, a mutation of Tyr306$^{7.53}$ does not influence the wild-type chemical shift for the Cβ of Cys187^{EL2}.

Discussion

The current study addresses several open questions regarding how retinal isomerization on the extracellular side of rhodopsin is coupled to the cytoplasmic ionic lock. We show that the interactions of Arg135$^{3.50}$ with Met257$^{6.40}$, Tyr223$^{5.58}$, and Tyr306$^{7.53}$ observed in the opsin crystal structure are also present in the active Meta II intermediate, consistent with the outward rotation of H6 (9, 12). Mutational studies indicate that the Arg135$^{3.50}$-Tyr223$^{5.58}$ interaction, which is facilitated by group-conserved Ala132$^{3.47}$, has a strong influence on the stability of the active state conformation.

Defining the Open and Closed States of the Glu134$^{3.49}$-Arg135$^{3.50}$-Glu247$^{6.30}$ Ionic Lock. The ionic lock was originally described as a conserved hydrophobic cage motif in the gonadotropin-releasing hormone receptor at the cytoplasmic end of H3 involving Asp$^{3.49}$, Arg$^{3.50}$, and Ile$^{3.54}$ (29). Ballesteros et al. (29) proposed that a salt bridge between Asp$^{3.49}$ and Arg$^{3.50}$ stabilizes the inactive receptor and that upon activation Asp$^{3.49}$ becomes protonated with the charged Arg$^{3.50}$ side chain being prevented from orienting toward the cytoplasmic surface by Ile$^{3.54}$. A more complex ionic lock involving the interaction of Arg$^{3.50}$ with both Asp$^{3.49}$ and Glu$^{6.30}$ was based on the observation of increased basal activity in the D3.49N and E6.30Q mutants of the β_2 adrenergic receptor (30). In the past few years, however, the crystal structures of the adenosine A2a (31) and β_1 (32) and β_2 (33) adrenergic receptors have been determined and, in contrast to rhodopsin, show no direct interaction between Arg$^{3.50}$ and Glu$^{6.30}$, although the Asp$^{3.49}$-Arg$^{3.50}$ salt bridge is retained.

Our results provide insights into the nature of the closed and open states of the ionic lock. Table S1 presents a summary of the conservation of the residues contributing to the ionic lock in rhodopsin and Meta II. There is a strong conservation of

Glu/Asp (90%) at position 3.49 and Arg (97%) at position 3.50. In contrast, Glu247$^{6.30}$ is not well conserved (33%) across the class A GPCRs, implying that there are various mechanisms for stabilizing inactive conformations. In the β_1 and β_2 adrenergic receptors, the position of Arg$^{3.50}$ is stabilized by a tyrosine on cytoplasmic loop 2, whose conservation in the amine subfamily (85%) is as high as the conservation of Glu$^{6.30}$ (83%). The conservation of two different residues that may stabilize Arg$^{3.50}$ in the amine receptors suggests that there may be multiple inactive states as seen in molecular dynamics (MD) simulations (34) or that these residues have other functions in the regulation of receptor activity (35).

Table S2 summarizes the conservation of residues stabilizing the active conformation of Arg135$^{3.50}$. The conservation of Tyr223$^{5.58}$ (86%) is striking because it is oriented toward the lipid in the dark state of rhodopsin, implying that it has only protein contacts in the active state. In contrast, Met at position 6.40 is not conserved in the class A GPCRs yet plays an important role in stabilizing the inactive conformation of rhodopsin (see below). Together, these observations support the view that the Glu134$^{3.49}$-Arg135$^{3.50}$ salt bridge is the essential interaction for stabilizing the inactive state of class A GPCRs (36). Neutralization of Glu134$^{3.49}$, rather than breaking of the Arg135$^{3.50}$-Glu247$^{6.30}$ salt bridge, is key to shifting the receptor to its active conformation where the conserved interactions are between Arg$^{3.50}$, Tyr$^{5.58}$, and Tyr$^{7.53}$, as observed in Meta II and the crystal structure of opsin.

Met257$^{6.40}$ Stabilizes Rhodopsin in the Inactive State. We had previously observed that most site-directed mutants of Met257$^{6.40}$ allow opsin activation by the addition of *all-trans*-retinal as a diffusible ligand (37). The observation that Met257$^{6.40}$ shifts into contact with Arg135$^{3.50}$ in the H3–H6 interface provides an explanation for the Met257$^{6.40}$ mutations and the role of Met257$^{6.40}$ in activation. The Met257$^{6.40}$ mutants with the highest constitutive activity are M257Y, M257N, and M257S. The polar side chains at position 6.40 in these mutants interact more strongly with Arg135$^{3.50}$ than the hydrophobic Met side chain and consequently stabilize the active state. In other class A GPCRs (Table S2), the β-branched amino acids (Thr, Ile, and Val) are the most common residues observed at position 6.40. When substituted into rhodopsin (37), these residues do not confer appreciable constitutive receptor activity (4.4–9.6%) but do allow almost full activation (62–83%) upon the addition of *all-trans*-retinal. These results indicate that, rather than stabilizing the active state, Met257$^{6.40}$ stabilizes the inactive state of the receptor. If Met257$^{6.40}$ is not stabilizing the Meta II structure, the question arises as to the relative stabilizing effects of Tyr223$^{5.58}$ and Tyr306$^{7.53}$. When these two tyrosines are mutated individually to phenylalanine, our measurements of transducin activation and Meta II decay indicate that Tyr223$^{5.58}$ plays a much greater role in stabilizing Meta II than Tyr306$^{7.53}$.

Ala132$^{3.47}$ Serves as a Molecular Notch for Tyr223$^{5.58}$. In the class A GPCRs, there are 13 group-conserved residues that are located mainly in the interfaces between helices H1–H4 (24). Importantly, Ala132$^{3.47}$ does not fit this pattern. Ala132$^{3.47}$ is located on H3 but oriented toward the H5–H6 interface. The results described above, in combination with the opsin structure, provide an explanation for the high group conservation (99%) of this residue. Whereas the group-conserved amino acids mainly mediate helix–helix interactions in the inactive state of rhodopsin, Ala132$^{3.47}$ acts as a molecular notch to orient the Tyr223$^{5.58}$ side chain efficiently toward Arg135$^{3.50}$ and stabilize the active Meta II intermediate (Fig. 1).

Alanine is highly conserved (68% identity) at position 3.47 in the rhodopsin subfamily of class A GPCRs. In the amine subfamily this site is predominantly a serine (68% identity). In the β_2-adrenergic receptor, we previously studied the influence of substitution of the group-conserved amino acids in the TM-helix core with larger hydrophobic residues (38). Substitution of the wild-type Ala at position 3.47 with Leu or Val dramatically lowered receptor activity, whereas Ser at position 3.47 exhibited wild-type activity, suggesting that the role of Ala132$^{3.47}$ in rhodopsin is likely the same across the class A GPCRs. In the recent crystal structures of both the β_2-adrenergic and A2a receptors, Tyr$^{5.58}$ has rotated toward Ala$^{3.47}$, as in activated opsin. This active orientation for Tyr$^{5.58}$ may be due to the T4 lysozyme (T4L) insert between H5 and H6 used to crystallize both receptors. Comparison with the wild-type receptors shows that the T4L insert results in higher affinity for subtype-selective agonists, which the authors suggest may reflect a shift toward the active state (31, 33). In addition, MD simulations of the β_2 receptor without the T4L insert show rapid formation of the Arg$^{3.50}$-Glu$^{6.40}$ interaction (34). In the β_1 receptor, which was not crystallized with the T4L insert, Tyr$^{5.58}$ was mutated to alanine as part of a suite of mutations engineered to stabilize the inactive conformation of the receptor (32).

Allosteric Coupling Across the Transmembrane Core of Rhodopsin. Solid-state NMR measurements have previously suggested that the displacement of EL2 upon activation is coupled to rotation of H5 (17). The coupled motion of EL2 and H5 was based on mutational experiments where substitutions in EL2 resulted in structural changes in H5 (17). Here, we show that mutations in H5 (i.e., Y223F) result in structural changes in EL2 (i.e., Cys187^{EL2}). In agreement with previous studies on Cys187^{EL2} (39), mutation of Tyr223$^{5.58}$ does not affect the wild-type properties of rhodopsin in the dark but leads to a less stable Meta II intermediate upon activation. In wild-type rhodopsin at neutral pH, hydrolysis of the *all-trans*-retinal SB and loss of the retinal chromophore in the Meta II to opsin transition shifts the receptor to an inactive conformation (11). Inactive opsin is stabilized, at least in part, by electrostatic interactions involving Glu113$^{3.28}$ and Lys296$^{7.43}$ because mutation of either residue to a neutral amino acid increases constitutive receptor activity (40). Interestingly, in the active opsin structure (12), these residues do not interact directly but rather interact most closely with Cys187^{EL2} and Glu181^{EL2}, respectively, on EL2. Coupling of the position of EL2 to the orientation of H5 in the Meta II to opsin transition would suggest that there is a role for Tyr223$^{5.58}$ in both the opening and closing of the Arg135$^{3.50}$-Glu134$^{3.49}$ ionic lock.

In summary, the current study highlights the roles of several residues mediating the opening and closing of the ionic lock in rhodopsin activation. The observed active state contacts of Arg135$^{3.50}$ with Met257$^{6.40}$, Tyr223$^{5.58}$, and Tyr306$^{7.53}$ allow us to define the open conformation of the ionic lock. In particular, we show that a unique interaction between Tyr223$^{5.58}$ and Ala132$^{3.47}$ in the active Meta II intermediate can explain both the high sequence identity of Tyr223$^{5.58}$ and the high group conservation of Ala132$^{3.47}$ across the class A GPCRs.

Methods

Materials. ^{13}C-labeled amino acids were purchased from Cambridge Isotope Laboratories.

Expression and Purification of ^{13}C-Labeled Rhodopsin. Stable tetracycline-inducible HEK293S cell lines containing the opsin (bovine) gene and its mutants was used to express rhodopsin. The expression and purification in *n*-dodecyl maltoside (DDM) have previously been described (16, 17).

Transducin Activity. The reaction mixture containing mutant rhodopsin (20 nM) and transducin (250 nM) in 10 mM Tris, pH 7.2, 2 mM $MgCl_2$, 100 mM NaCl, 1 mM dithiothreitol, and 0.012% (wt/vol) DDM was illuminated by using a 495-nm long pass filter at 20 °C with constant stirring. The reaction was initiated by the addition of 5 μM GTPγS, and the fluorescence was monitored for 2,000 s. The sample was excited at 295 nm (2 nm

bandwidth) and emission was monitored at 340 nm (15 nm bandwidth) at 3-s intervals with an integration time of 2 s. Initial rates were calculated by using the data points collected over the first 60 s following GTP addition.

Fluorescence Spectroscopy. Meta II decay was monitored by using a fluorescence-based assay (19). Rhodopsin (250 nM) was illuminated by using a 495-nm long pass filter at 20 °C in 10 mM 1,3-bis[tris(hydroxymethyl)methylamino]propane, pH 6 containing 0.1% (wt/vol) DDM. The fluorescence was monitored every 30 s for 7,200 s by using a 2-s integration time. Samples were excited at 280 nm (2 nm bandwidth) and emission measured at 330 nm (15 nm bandwidth).

Solid-State NMR Spectroscopy. Solid-state ^{13}C magic angle spinning spectra were acquired at a static magnetic field strength of 14.1 T (600 MHz) on a Bruker AVANCE spectrometer as previously described (16, 17). NMR spectra were obtained at 190 K by using rhodopsin or Meta II solubilized in DDM.

ACKNOWLEDGMENTS. This work was supported by National Institutes of Health–National Science Foundation instrumentation grants (S10 RR13889 and DBI-9977553), National Institutes of Health Grant GM-41412 (to S.O.S.), and Deutsche Forschungsgemeinschaft Grant Za 566/2-1 (to E.Z.) and Grant Vo 811/4-1 (to R.V.). We gratefully acknowledge the W.M. Keck Foundation for support of the NMR facilities in the Center of Structural Biology at Stony Brook.

1. Ballesteros JA, Weinstein H (1995) Integrated methods for the construction of three dimensional models and computational probing of structure-function relations in G-protein coupled receptors. *Methods Neurosci* 25:366–428.
2. Palczewski K, et al. (2000) Crystal structure of rhodopsin: A G protein-coupled receptor. *Science* 289:739–745.
3. Altenbach C, Kusnetzow AK, Ernst OP, Hofmann KP, Hubbell WL (2008) High-resolution distance mapping in rhodopsin reveals the pattern of helix movement due to activation. *Proc Natl Acad Sci USA* 105:7439–7444.
4. Farrens DL, Altenbach C, Yang K, Hubbell WL, Khorana HG (1996) Requirement of rigid-body motion of transmembrane helices for light activation of rhodopsin. *Science* 274:768–770.
5. Lamola AA, Yamane T, Zipp A (1974) Effects of detergents and high-pressures upon metarhodopsin I ↔ metarhodopsin II equilibrium. *Biochemistry* 13:738–745.
6. Okada T, Palczewski K (2001) Crystal structure of rhodopsin: Implications for vision and beyond. *Curr Opin Struct Biol* 11:420–426.
7. Salom D, et al. (2006) Crystal structure of a photoactivated deprotonated intermediate of rhodopsin. *Proc Natl Acad Sci USA* 103:16123–16128.
8. Knierim B, Hofmann KP, Ernst OP, Hubbell WL (2007) Sequence of late molecular events in the activation of rhodopsin. *Proc Natl Acad Sci USA* 104:20290–20295.
9. Park JH, Scheerer P, Hofmann KP, Choe HW, Ernst OP (2008) Crystal structure of the ligand-free G-protein-coupled receptor opsin. *Nature* 454:183–187.
10. Jäger S, Palczewski K, Hofmann KP (1996) Opsin/all-trans-retinal complex activates transducin by different mechanisms than photolyzed rhodopsin. *Biochemistry* 35:2901–2908.
11. Vogel R, Siebert F (2001) Conformations of the active and inactive states of opsin. *J Biol Chem* 276:38487–38493.
12. Scheerer P, et al. (2008) Crystal structure of opsin in its G-protein-interacting conformation. *Nature* 455:497–502.
13. Kisselev OG, et al. (1998) Light-activated rhodopsin induces a structural binding motif in G protein α subunit. *Proc Natl Acad Sci USA* 95:4270–4275.
14. Koenig BW, et al. (2002) Structure and orientation of a G protein fragment in the receptor bound state from residual dipolar couplings. *J Mol Biol* 322:441–461.
15. Fritze O, et al. (2003) Role of the conserved NPxxY(x)(5,6)F motif in the rhodopsin ground state and during activation. *Proc Natl Acad Sci USA* 100:2290–2295.
16. Ahuja S, et al. (2009) Location of the retinal chromophore in the activated state of rhodopsin. *J Biol Chem* 284:10190–10201.
17. Ahuja S, et al. (2009) Helix movement is coupled to displacement of the second extracellular loop in rhodopsin activation. *Nat Struct Mol Biol* 16:168–175.
18. Petkova AT, et al. (1999) Arginine activity in the proton-motive photocycle of bacteriorhodopsin: Solid-state NMR studies of the wild-type and D85N proteins. *Biochemistry* 38:1562–1572.
19. Farrens DL, Khorana HG (1995) Structure and function in rhodopsin. Measurement of the rate of metarhodopsin II decay by fluorescence spectroscopy. *J Biol Chem* 270:5073–5076.
20. Andres A, Garriga P, Manyosa J (2003) Altered functionality in rhodopsin point mutants associated with retinitis pigmentosa. *Biochem Biophys Res Commun* 303:294–301.
21. Hawtin SR (2005) Charged residues of the conserved DRY triplet of the vasopressin V1a receptor provide molecular determinants for cell surface delivery and internalization. *Mol Pharmacol* 68:1172–1182.
22. Auger GA, Pease JE, Shen XY, Xanthou G, Barker MD (2002) Alanine scanning mutagenesis of CCR3 reveals that the three intracellular loops are essential for functional receptor expression. *Eur J Immunol* 32:1052–1058.
23. Eilers M, Patel AB, Liu W, Smith SO (2002) Comparison of helix interactions in membrane and soluble α-bundle proteins. *Biophys J* 82:2720–2736.
24. Smith SO (2010) Structure and activation of the visual pigment rhodopsin. *Annu Rev Biophys* 39:309–328.
25. Imai H, et al. (1997) Single amino acid residue as a functional determinant of rod and cone visual pigments. *Proc Natl Acad Sci USA* 94:2322–2326.
26. Patel AB, et al. (2005) Changes in interhelical hydrogen bonding upon rhodopsin activation. *J Mol Biol* 347:803–812.
27. Janz JM, Farrens DL (2004) Role of the retinal hydrogen bond network in rhodopsin Schiff base stability and hydrolysis. *J Biol Chem* 279:55886–55894.
28. Sakmar TP, Franke RR, Khorana HG (1989) Glutamic acid-113 serves as the retinylidene Schiff base counterion in bovine rhodopsin. *Proc Natl Acad Sci USA* 86:8309–8313.
29. Ballesteros J, et al. (1998) Functional microdomains in G-protein-coupled receptors—the conserved arginine-cage motif in the gonadotropin-releasing hormone receptor. *J Biol Chem* 273:10445–10453.
30. Ballesteros JA, et al. (2001) Activation of the β_2-adrenergic receptor involves disruption of an ionic lock between the cytoplasmic ends of transmembrane segments 3 and 6. *J Biol Chem* 276:29171–29177.
31. Jaakola VP, et al. (2008) The 2.6 Angstrom crystal structure of a human A_{2A} adenosine receptor bound to an antagonist. *Science* 322:1211–1217.
32. Warne T, et al. (2008) Structure of a β_1-adrenergic G-protein-coupled receptor. *Nature* 454:486–491.
33. Rosenbaum DM, et al. (2007) GPCR engineering yields high-resolution structural insights into β_2-adrenergic receptor function. *Science* 318:1266–1273.
34. Dror RO, et al. (2009) Identification of two distinct inactive conformations of the β_2-adrenergic receptor reconciles structural and biochemical observations. *Proc Natl Acad Sci USA* 106:4689–4694.
35. Baltensperger K, et al. (1996) The β-adrenergic receptor is a substrate for the insulin receptor tyrosine kinase. *J Biol Chem* 271:1061–1064.
36. Vogel R, et al. (2008) Functional role of the "ionic lock"—an interhelical hydrogen-bond network in family a heptahelical receptors. *J Mol Biol* 380:648–655.
37. Han M, Smith SO, Sakmar TP (1998) Constitutive activation of opsin by mutation of methionine 257 on transmembrane helix 6. *Biochemistry* 37:8253–8261.
38. Chelikani P, et al. (2007) Role of group-conserved residues in the helical core of β_2-adrenergic receptor. *Proc Natl Acad Sci USA* 104:7027–7032.
39. Davidson FF, Loewen PC, Khorana HG (1994) Structure and function in rhodopsin: Replacement by alanine of cysteine residues 110 and 187, components of a conserved disulfide bond in rhodopsin, affects the light-activated metarhodopsin II state. *Proc Natl Acad Sci USA* 91:4029–4033.
40. Cohen GB, Oprian DD, Robinson PR (1992) Mechanism of activation and inactivation of opsin: Role of Glu113 and Lys296. *Biochemistry* 31:12592–12601.